



HAL
open science

Altered skeletal muscle lipase expression and activity contribute to insulin resistance in humans.

Pierre-Marie Badin, Katie Louche, Aline Mairal, Gerhard Liebisch, Gerd Schmitz, Arild C. Rustan, Steven R. Smith, Dominique Langin, Cedric Moro

► **To cite this version:**

Pierre-Marie Badin, Katie Louche, Aline Mairal, Gerhard Liebisch, Gerd Schmitz, et al.. Altered skeletal muscle lipase expression and activity contribute to insulin resistance in humans.. *Diabetes*, 2011, 60 (6), pp.1734-42. 10.2337/db10-1364 . inserm-00726449

HAL Id: inserm-00726449

<https://inserm.hal.science/inserm-00726449>

Submitted on 30 Aug 2012

HAL is a multi-disciplinary open access archive for the deposit and dissemination of scientific research documents, whether they are published or not. The documents may come from teaching and research institutions in France or abroad, or from public or private research centers.

L'archive ouverte pluridisciplinaire **HAL**, est destinée au dépôt et à la diffusion de documents scientifiques de niveau recherche, publiés ou non, émanant des établissements d'enseignement et de recherche français ou étrangers, des laboratoires publics ou privés.

Altered Skeletal Muscle Lipase Expression and Activity Contribute to Insulin Resistance in Humans

Pierre-Marie Badin,^{1,2} Katie Louche,^{1,2} Aline Mairal,^{1,2} Gerhard Liebisch,³ Gerd Schmitz,³ Arild C. Rustan,⁴ Steven R. Smith,⁵ Dominique Langin,^{1,2,6} and Cedric Moro^{1,2}

OBJECTIVE—Insulin resistance is associated with elevated content of skeletal muscle lipids, including triacylglycerols (TAGs) and diacylglycerols (DAGs). DAGs are by-products of lipolysis consecutive to TAG hydrolysis by adipose triglyceride lipase (ATGL) and are subsequently hydrolyzed by hormone-sensitive lipase (HSL). We hypothesized that an imbalance of ATGL relative to HSL (expression or activity) may contribute to DAG accumulation and insulin resistance.

RESEARCH DESIGN AND METHODS—We first measured lipase expression in vastus lateralis biopsies of young lean ($n = 9$), young obese ($n = 9$), and obese-matched type 2 diabetic ($n = 8$) subjects. We next investigated in vitro in human primary myotubes the impact of altered lipase expression/activity on lipid content and insulin signaling.

RESULTS—Muscle ATGL protein was negatively associated with whole-body insulin sensitivity in our population ($r = -0.55$, $P = 0.005$), whereas muscle HSL protein was reduced in obese subjects. We next showed that adenovirus-mediated ATGL overexpression in human primary myotubes induced DAG and ceramide accumulation. ATGL overexpression reduced insulin-stimulated glycogen synthesis (-30% , $P < 0.05$) and disrupted insulin signaling at Ser1101 of the insulin receptor substrate-1 and downstream Akt activation at Ser473. These defects were fully rescued by nonselective protein kinase C inhibition or concomitant HSL overexpression to restore a proper lipolytic balance. We show that selective HSL inhibition induces DAG accumulation and insulin resistance.

CONCLUSIONS—Altogether, the data indicate that altered ATGL and HSL expression in skeletal muscle could promote DAG accumulation and disrupt insulin signaling and action. Targeting skeletal muscle lipases may constitute an interesting strategy to improve insulin sensitivity in obesity and type 2 diabetes. *Diabetes* 60:1734–1742, 2011

Skeletal muscle insulin resistance is a strong risk factor of type 2 diabetes and cardiovascular diseases (1,2). Dysfunctional adipose tissue can lead to lipid oversupply and increased flux of free fatty acids (FFAs) into skeletal muscle and is associated with the accumulation of intramyocellular triacylglycerols (IMTGs) (3–5). This chronic lipid overload in tissues can evolve to a state of lipotoxicity leading to cell dysfunction (6). The term “lipotoxicity” defines more generally in skeletal muscle a state of lipid overload (increased concentrations of long-chain acyl-CoA, diacylglycerols [DAGs], and ceramide) causing insulin resistance (7–12). DAGs have been shown to activate novel protein kinase C (PKC) isoforms, such as the novel PKC θ leading to insulin receptor substrate-1 (IRS-1) serine phosphorylation and impaired downstream insulin signaling (10–13). DAGs can be formed through multiple pathways but are also formed as intermediates during triacylglycerol (TAG) synthesis and hydrolysis (14). The control of lipolysis in skeletal muscle has mainly been attributed to hormone-sensitive lipase (HSL), which exhibits a 10-fold higher specific activity for DAG than TAG (15). HSL null mice display normal TAG hydrolase activity after an overnight fast and accumulate large amounts of DAG (16). Recently it was shown that adipose triglyceride lipase (ATGL) plays a major role in the regulation of cellular TAG stores in various tissues of the body, including heart and skeletal muscle (17,18). ATGL specifically drives the hydrolysis of TAG into DAG (18). ATGL-deficient mice are more insulin sensitive and glucose tolerant despite a threefold increase in TAG content in their skeletal muscle (17). The molecular mechanism underlying this phenotype remains unclear. In the current study, we hypothesized that an imbalance of ATGL relative to HSL could increase intracellular DAG concentrations and promote insulin resistance. To test this hypothesis, we first examined the relationship between muscle ATGL expression and whole-body insulin sensitivity in a wide range of subjects. We next manipulated the expression/activity of ATGL and HSL in vitro in cultured human primary skeletal muscle cells and evaluated its impact on lipid pools and insulin signaling.

RESEARCH DESIGN AND METHODS

Skeletal muscle cell culture. Satellite cells from vastus lateralis or rectus abdominis biopsies of lean, healthy, insulin-sensitive subjects were isolated by trypsin digestion, preplated on an uncoated petri dish for 1 h to remove fibroblasts, and subsequently transferred to T-25 collagen-coated flasks in Dulbecco's modified Eagle's medium (DMEM) low glucose (1 g/L) supplemented with 10% FBS and growth factors (human epidermal growth factor, BSA, dexamethasone, gentamicin, amphotericin B [Fungizone, Invitrogen, Grand Island, NY], and fetuin) as previously described (19). Cells from several donors were pooled and grown at 37°C in a humidified atmosphere of 5% CO₂. Differentiation of myoblasts into myotubes was initiated at approximately 90% confluence by switching to α -minimum essential medium with antibiotics,

From ¹INSERM, U1048, Obesity Research Laboratory, Institute of Metabolic and Cardiovascular Diseases (I2MC), Toulouse, France; the ²Paul Sabatier University, University of Toulouse, Toulouse, France; the ³Institute of Clinical Chemistry, University of Regensburg, Regensburg, Germany; the ⁴Department of Pharmaceutical Biosciences, School of Pharmacy, University of Oslo, Oslo, Norway; the ⁵Translational Research Institute for Metabolism and Diabetes and the Burnham Institute, Florida Hospital, Winter Park, Florida; and the ⁶Centre Hospitalier Universitaire de Toulouse, Biochemistry Laboratory, Biology Institute of Purpan, Toulouse, France.

Corresponding author: Cedric Moro, cedric.moro@inserm.fr.

Received 24 September 2010 and accepted 3 March 2011.

DOI: 10.2337/db10-1364

This article contains Supplementary Data online at <http://diabetes.diabetesjournals.org/lookup/suppl/doi:10.2337/db10-1364/-/DC1>.

© 2011 by the American Diabetes Association. Readers may use this article as long as the work is properly cited, the use is educational and not for profit, and the work is not altered. See <http://creativecommons.org/licenses/by-nc-nd/3.0/> for details.

2% FBS, and fetuin. The medium was changed every other day, and cells were grown up to 5–6 days.

Overexpression of lipases. Human ATGL and HSL cDNAs were cloned into the pcDNA3 vector (Invitrogen Corp., Carlsbad, CA). DNA sequencing was performed to check correct insertion of the cDNA using an ABI3100 automatic sequencer (Applied Biosystems, Courtaboeuf, France). Adenoviruses expressing in tandem green fluorescent protein (GFP) and ATGL or HSL were constructed, purified, and titrated (Vector Biolabs, Philadelphia, PA). An adenovirus containing the GFP gene only was used as a control. Myotubes were infected with the control (GFP), ATGL, and HSL adenoviruses at day 4 of differentiation and remained exposed to the virus for 24 h in serum-free DMEM containing 150 $\mu\text{mol/L}$ of oleate complexed to BSA (ratio 4:1). Oleate was preferred to palmitate for lipid loading of the cells to favor TAG synthesis and to avoid the intrinsic lipotoxic effect of palmitate (20,21). No adenovirus-induced cellular toxicity was observed as determined by chemiluminescent quantification of adenylate kinase activity (ToxiLight, Lonza Group Ltd., Basel, Switzerland). For insulin signaling experiments, infected myotubes were incubated for 20 min in DMEM low glucose with or without 100 nmol/L of insulin (Sigma-Aldrich, Lyon, France).

Determination of glycogen synthesis. Cells were preincubated with a glucose- and serum-free α -minimum essential medium for 90 min and then exposed to DMEM supplemented with $[U-^{14}\text{C}]$ glucose (1 $\mu\text{Ci/mL}$; PerkinElmer, Boston, MA) in the presence or absence of 100 nmol/L insulin for 3 h. After incubation, glycogen synthesis was determined as described previously (22).

Pulse-chase studies of lipid metabolism. Cells were pulsed overnight (18 h) with a combination of $[1-^{14}\text{C}]$ oleate (1 $\mu\text{Ci/mL}$; PerkinElmer) and unlabeled oleate (100 $\mu\text{mol/L}$ final concentration) to prelabel the endogenous TAG pool. After incubation, myotubes were chased for 3 h in nutrient-deficient DMEM containing 0.1 mmol/L glucose and 0.5% FFA-free BSA. At the end of incubation, total lipids were extracted in chloroform/methanol (2v/1v) and separated by thin-layer chromatography as previously described (23). Incorporation rates were normalized to total protein content measured in each well.

Western blot analysis. Muscle tissues and cell extracts were homogenized in a buffer containing 50 mmol/L HEPES, pH 7.4, 2 mmol/L EDTA, 150 mmol/L NaCl, 30 mmol/L NaPO_4 , 10 mmol/L NaF, 1% Triton X-100, 10 $\mu\text{L/mL}$ protease inhibitor (Sigma-Aldrich), 10 $\mu\text{L/mL}$ phosphatase I inhibitor (Sigma-Aldrich), 10 $\mu\text{L/mL}$ phosphatase II inhibitor (Sigma-Aldrich), and 1.5 mg/mL benzamide HCl. Tissue homogenates were centrifuged for 25 min at 15,000g, and supernatants were stored at -80°C . Solubilized proteins from muscle tissue and myotubes were run on a 4–12% SDS-PAGE (Bio-Rad, Hercules, CA), transferred onto nitrocellulose membrane (Hybond ECL, GE Healthcare, Buckinghamshire, U.K.), and incubated with the primary antibodies (ATGL, Cell Signaling Technology Inc., Beverly, MA; Perilipin-A, Abcam Inc., Cambridge, MA). The HSL antibody was as previously described (24). Antibodies for insulin signaling *p*-Ser473–Akt, Akt, *p*-Ser1101–IRS-1, *p*-Tyr612–IRS-1, IRS-1, and *p*-Ser660–HSL were all from Cell Signaling Technology Inc. Subsequently, immunoreactive proteins were determined by enhanced chemiluminescence reagent (GE Healthcare, Waukesha, WI) and visualized by exposure to Hyperfilm ECL (GE Healthcare). Glyceraldehyde-3-phosphate dehydrogenase (GAPDH) (Cell Signaling Technology Inc.) served as an internal control.

Subjects. Nine young lean, nine young obese, and eight obese subjects with type 2 diabetes were recruited in the study (Table 1). The subjects with type 2 diabetes were diet-controlled or were taking metformin ($n = 6$) and insulin ($n = 2$), and were otherwise healthy with an average HbA_{1c} of $7.0 \pm 0.78\%$. None of them were taking thiazolidinediones. The protocol was approved by

the institutional review board of the Pennington Biomedical Research Center, and all volunteers gave written informed consent. After participants completed the screening visit, fat mass was measured on a Hologic Dual Energy X-Ray Absorptiometer (QDR 2000, Hologic Inc., Bedford, MA). The participants were asked to refrain from vigorous physical activity for 48 h before presenting to the Pennington inpatient clinic and ate a weight-maintaining diet consisting of 35% fat, 16% protein, and 49% carbohydrate 2 days before the clamp and the muscle biopsy. Samples of vastus lateralis weighing 60–100 mg were obtained by muscle biopsy using the Bergstrom technique, blotted, cleaned, and snap-frozen in liquid nitrogen (25).

Hyperinsulinemic euglycemic clamp. Insulin sensitivity was measured by clamp (26). After an overnight fast, insulin ($80 \text{ mU} \cdot \text{m}^{-2} \cdot \text{min}^{-1}$) and 20% glucose (to maintain plasma glucose at 90 mg/dL) were administered for 2 h. Glucose and insulin were measured in three independent blood plasma samples 5 min apart at baseline and again at steady-state after approximately 2 h. Glucose disposal rate was adjusted for kilograms of fat-free mass.

Lipase activity assays. TAG hydrolase (TAGH) and DAG hydrolase (DAGH) activities were measured on cell extracts as previously described (24,27). Briefly, 1(3)-mono[^3H]oleyl-2-*O*-mono-oleylglycerol (MOME) and [9, 10- ^3H (N)]triolein were emulsified with phospholipids by sonication. MOME is a DAG analog that allows for the measurement of DAGH activity because it is not a substrate for monoacylglycerol lipase. [9, 10- ^3H (N)]triolein was used to determine specifically TAGH activity, and [^3H]MOME was used to determine specifically DAGH activity.

TAG and DAG determination by gas chromatography-mass spectrometry. Total lipids were extracted from frozen muscle tissue samples and from myotubes harvested in water containing 0.25 mL 0.1% SDS. Lipids were extracted using the method of Folch et al. (28). The extracts were filtered, and lipids were recovered in the chloroform phase. TAG and DAG were isolated using thin-layer chromatography on Silica Gel 60 A plates developed in petroleum ether, ethyl ether, and acetic acid (80:20:1), and visualized by rhodamine 6G. The TAG and DAG band was scraped from the plate and methylated using BF_3 /methanol as described by Morrison and Smith (29). The methylated FFAs were extracted with hexane and analyzed by gas chromatography using an HP 5890 gas chromatograph equipped with flame ionization detectors, an HP 3365 Chemstation, and a capillary column (SP2380, 0.25 mm \times 30 m, 0.25 μm film; Supelco, Bellefonte, PA). Helium was used as a carrier gas. The oven temperature was programmed from 160 to 230°C at 4°C/min. FFA methyl esters were identified by comparing the retention times with those of known standards. Inclusion of the internal standards, 20:1 (tricosenoic) and 17:0 (diheptadecanoic), permits quantitation of the amount of TAG and DAG in the sample.

Ceramide determination by electrospray ionization tandem mass spectrometry. Ceramide was quantified by electrospray ionization tandem mass spectrometry as previously described (30). Briefly, lipid extracts were prepared by the method of Bligh and Dyer (31) in the presence of nonnaturally occurring Cer 14:0, Cer 17:0. Samples were analyzed by direct flow injection on a Quattro Ultima triple-quadrupole mass spectrometer (Micromass, Manchester, U.K.) using an HTS PAL autosampler (CTC Analytics AG, Zwingen, Switzerland) and an Agilent 1100 binary pump (Agilent Technologies GmbH, Waldbronn, Germany) with a solvent mixture of methanol containing 10 mmol/L ammonium acetate and chloroform (3:1, v/v). A flow gradient was performed starting with a flow of 55 $\mu\text{L/min}$ for 6 s followed by 30 $\mu\text{L/min}$ for 1.0 min and an increase to 250 $\mu\text{L/min}$ for another 12 s. Ceramide was analyzed using a fragment of m/z 264 with *N*-heptadecanoyl-sphingosine as internal standard. Both ions $[\text{M}+\text{H}]^+$ and $[\text{M}+\text{H}-\text{H}_2\text{O}]^+$ were used, and quantification was achieved by calibration lines generated by addition of Cer 16:0, 18:0, 20:0, 24:1, 24:0 to tissue and cell samples, respectively. Correction of isotopic overlap of ceramide species and data analysis were performed by self-programmed Excel (Microsoft Corp., Redmond, WA) macros according to the principles described previously (32).

Statistical analyses. All statistical analyses were performed using GraphPad Prism 5.0 for Windows (GraphPad Software Inc., San Diego, CA). One-way ANOVA followed by Bonferroni post hoc tests and paired, two-tailed Student *t* tests were performed to determine differences between groups and treatments. Two-way ANOVA and Bonferroni post hoc tests were used when appropriate. Normal distribution of the data was tested using the Shapiro-Wilk normality test. The relationships between muscle ATGL protein and clinical variables were analyzed using Spearman rank correlations. All values in Figs. 1 to 7 and Table 1 are presented as mean \pm SEM. Statistical significance was set at $P < 0.05$.

RESULTS

Relationship between muscle ATGL and insulin sensitivity. We first investigated the relationship between skeletal muscle ATGL protein content and insulin sensitivity

TABLE 1
Clinical characteristics of the subjects

| | Lean (9) | Obese (9) | Type 2 diabetes (8) |
|-------------------------------|-----------------|------------------------------|--------------------------------|
| Sex (male/female) | 6/3 | 5/4 | 6/2 |
| Age (years) | 23.8 \pm 0.8 | 23.7 \pm 0.8 | 53.8 \pm 3.8 ^{b,e} |
| Body weight (kg) | 66.4 \pm 3.6 | 94.5 \pm 3.4 ^c | 102.4 \pm 4.2 ^c |
| BMI (kg/m^2) | 22.5 \pm 0.5 | 32.9 \pm 0.5 ^c | 35.4 \pm 1.7 ^c |
| Body fat (%) | 20.4 \pm 2.8 | 31.1 \pm 1.6 ^a | 37.5 \pm 2.9 ^b |
| GDR (mg/min/kg FFM) | 9.3 \pm 0.8 | 7.0 \pm 0.6 ^a | 5.3 \pm 0.6 ^c |
| Fasting glucose (mmol/L) | 4.67 \pm 0.12 | 4.81 \pm 0.13 ^a | 7.51 \pm 0.76 ^{b,d} |
| Fasting insulin (mU/L) | 8.4 \pm 1.2 | 13.2 \pm 1.1 ^a | 13.7 \pm 2.9 ^a |

Data are mean \pm SEM. FFM, fat-free mass; GDR, glucose disposal rate. ^a $P < 0.05$, ^b $P < 0.01$, ^c $P < 0.001$ vs. lean; ^d $P < 0.01$, ^e $P < 0.001$ vs. obese.

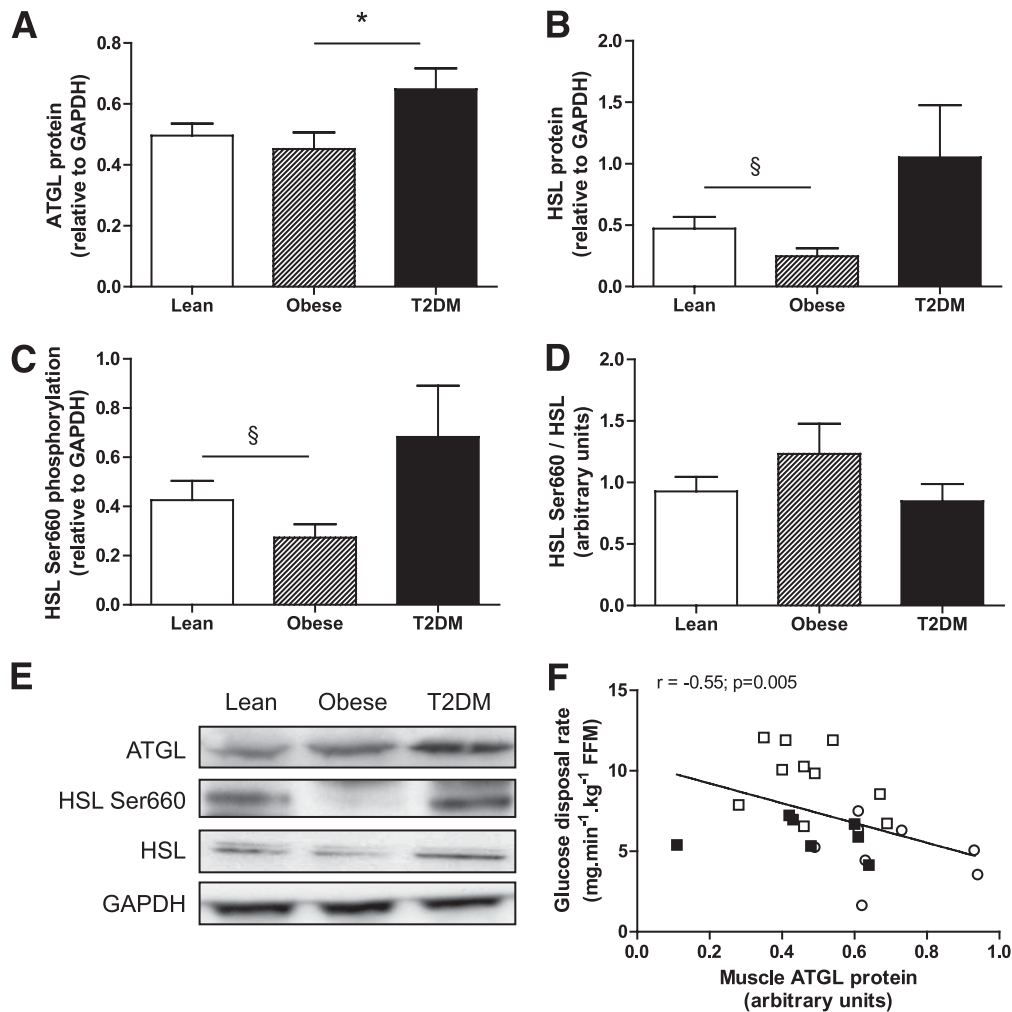


FIG. 1. Skeletal muscle lipase protein expression in lean, obese, and type 2 diabetic subjects. Quantitative bar graph of ATGL protein (A), HSL protein (B), HSL Ser660 phosphorylation (C), and the ratio HSL Ser660 phosphorylation to total HSL (D) in vastus lateralis samples of lean, obese, and type 2 diabetic subjects. E: Representative blots of lipases and the loading control GAPDH. F: Relationship between vastus lateralis ATGL protein expression and glucose disposal rate measured by euglycemic hyperinsulinemic clamp across individuals. White square, lean; black square, obese; open circle, type 2 diabetes. * $P < 0.05$ compared with obese; § $P = 0.08$ compared with lean.

in human vastus lateralis samples of young lean, young obese, and type 2 diabetic subjects. The characteristics of the subjects are described in Table 1. As expected, obese and type 2 diabetic subjects had lower insulin sensitivity and higher body fat, fasting glucose, and fasting insulin compared with lean subjects. Muscle ATGL protein content was significantly elevated in type 2 diabetic subjects when compared with lean and obese subjects (0.50 ± 0.04 , 0.45 ± 0.05 , and 0.65 ± 0.07 arbitrary units [AU] for lean, obese, and type 2 diabetic subjects, respectively) (Fig. 1A and E). We also confirm a reduced HSL Ser660 phosphorylation (0.43 ± 0.08 vs. 0.27 ± 0.05 AU, -36%) (Fig. 1C and E) and HSL protein content (0.47 ± 0.09 vs. 0.25 ± 0.07 AU, -48%) (Fig. 1B and E) in skeletal muscle of obese compared with lean subjects. HSL Ser660 phosphorylation (0.68 ± 0.21 vs. 0.43 ± 0.08 AU) and total HSL (1.05 ± 0.43 vs. 0.47 ± 0.09 AU) tended to increase in type 2 diabetic subjects compared with lean subjects. The ratio of phosphorylated HSL Ser660 to total HSL was not significantly changed between groups (Fig. 1D). We noted a significant inverse relationship between muscle ATGL protein content and whole-body insulin sensitivity measured by euglycemic hyperinsulinemic

clamp across individuals (Fig. 1F). Similarly, muscle ATGL protein was positively correlated with fasting glucose levels ($r = 0.56$, $P < 0.005$). Perilipin-A protein was not detectable in any of the muscle samples excluding significant contamination by infiltrated adipocytes (data not shown).

Adenovirus-mediated ATGL overexpression. We used an adenovirus gene delivery method to overexpress ATGL in our cell culture model. ATGL protein expression was induced by $\sim 3.4 \pm 0.2$ -fold (Fig. 2A). ATGL overexpression increased TAGH activity twofold (Fig. 2B), but did not change DAGH activity as expected (Fig. 2C). We checked that the ATGL enzyme was operative in intact cells by directly measuring the rate of incorporation of radiolabeled oleate into different lipid pools. We could show that ATGL overexpression reduced the rate of incorporation of [$1\text{-}^{14}\text{C}$] oleate into TAG (Fig. 2D), whereas the rate of incorporation was increased into DAG (Fig. 2E) and intracellular FFA (Fig. 2F).

Elevated ATGL expression promotes DAG and ceramide accumulation. We found that total TAG content was reduced in myotubes overexpressing ATGL (0.60 ± 0.07 -fold, $P < 0.01$) (Fig. 3A). Conversely, consistent with an

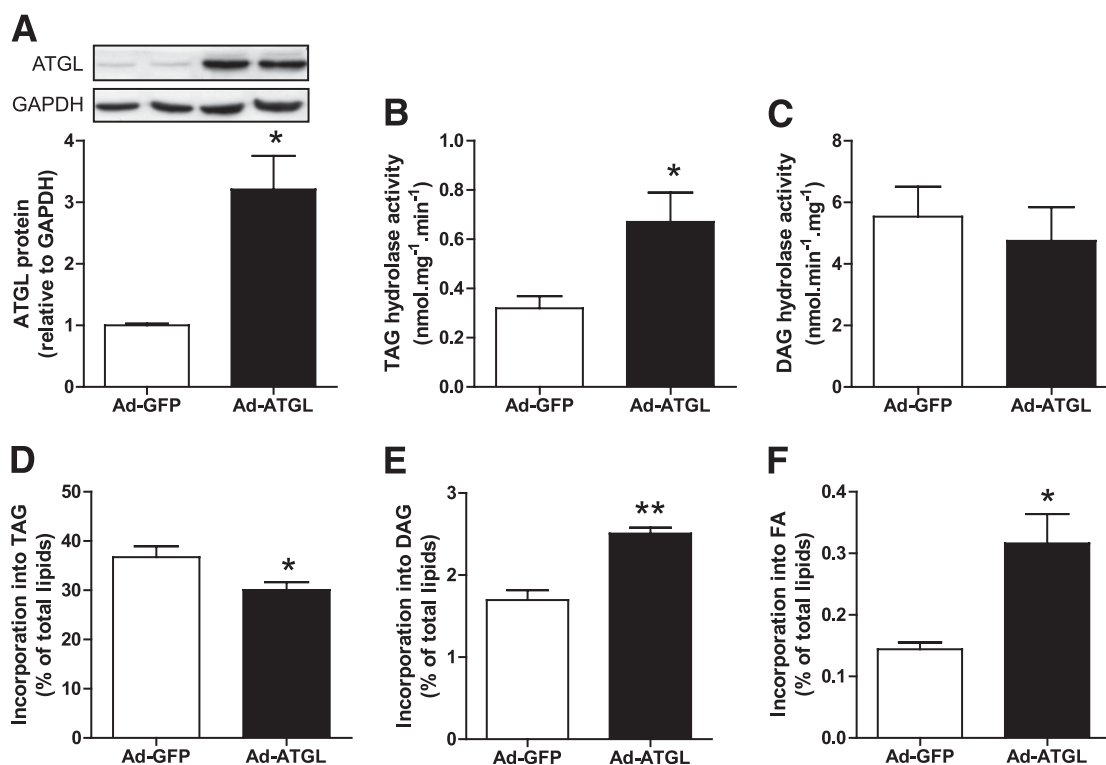


FIG. 2. ATGL overexpression increases TAG hydrolysis in myotubes. **A:** Quantitative bar graph of ATGL protein during adenovirus-mediated ATGL overexpression vs. GFP control ($n = 4$). Insets are showing representative blots of two independent experiments. TAG hydrolyse activity (**B**) and DAG hydrolyse activity (**C**) were measured in control myotubes (GFP) and myotubes overexpressing ATGL ($n = 4$). Pulse-chase studies using [^{14}C]oleate were performed to determine the kinetics of the different lipid pools in response to ATGL overexpression. The rate of incorporation of radiolabeled oleate into (**D**) TAG, (**E**) DAG, and (**F**) FFA was determined in control myotubes (GFP) and myotubes overexpressing ATGL. * $P < 0.05$; ** $P < 0.01$ vs. GFP ($n = 4$).

imbalance of ATGL relative to HSL, total DAG content increased in myotubes overexpressing ATGL (1.5 ± 0.1 -fold) (Fig. 3B). Ceramide content was also increased in myotubes overexpressing ATGL (2.9 ± 0.7 -fold), possibly as a consequence of increased intracellular FFA flux and de novo ceramide synthesis (Fig. 3C).

Elevated ATGL expression impairs insulin signaling and action. We first showed that glycogen synthesis under insulin stimulation was impaired by 30% ($P < 0.05$) in myotubes overexpressing ATGL (Fig. 4A). Insulin-stimulated glycogen synthesis was significantly reduced in myotubes overexpressing ATGL (0.72 ± 0.07 -fold, $P = 0.01$). We further showed that ATGL overexpression increased Ser1101-IRS-1 phosphorylation by twofold at baseline and under insulin stimulation ($P < 0.001$) (Fig. 4B and D). IRS-1 phosphorylation at Ser1101 inhibits IRS-1 tyrosine phosphorylation and

function and is a primary target for PKC (13), suggesting a possible link between ATGL and PKC activation. Downstream insulin activation of Akt on the residue Ser473 was also impaired (change insulin minus baseline -31% , $P < 0.05$) during ATGL overexpression. Ser473 Akt phosphorylation was increased at baseline ($P < 0.05$) and reduced under insulin stimulation in ATGL-overexpressing myotubes, whereas total Akt protein content was not different across treatments (Fig. 4C and D).

ATGL-mediated insulin resistance involves DAG and PKC activation. Because several isoforms of novel PKC have been linked to insulin resistance (33), we used a broad range nonselective PKC inhibitor in our experiments. Calphostin C treatment greatly enhanced insulin-stimulated Akt activation in ATGL overexpressing myotubes ($+163\%$, $P < 0.01$ compared with GFP with calphostin C)

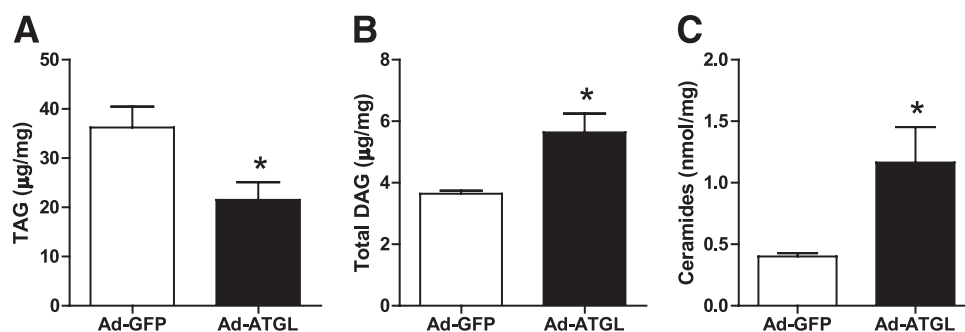


FIG. 3. Elevated ATGL expression promotes DAG and ceramide accumulation. Determination of (**A**) TAG, (**B**) DAG, and (**C**) ceramide content in control myotubes (GFP) and myotubes overexpressing ATGL. * $P < 0.05$ ($n = 5$).

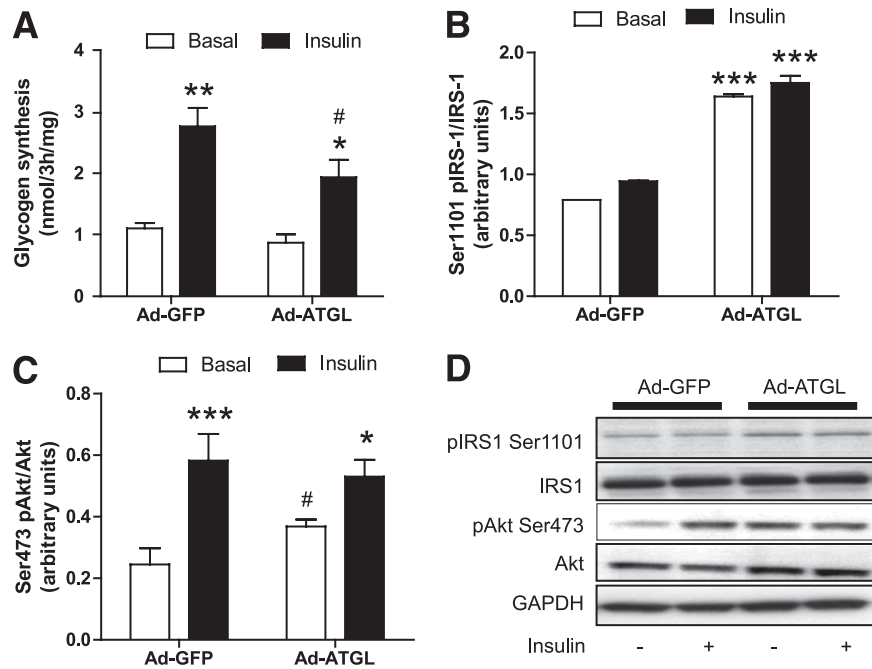


FIG. 4. Elevated ATGL expression disrupts insulin signaling and action. **A:** Glycogen synthesis was measured in the absence (open bars) or presence (black bars) of 100 nmol/L insulin in control myotubes (GFP) and myotubes overexpressing ATGL. * $P < 0.05$, ** $P < 0.01$ vs. basal; # $P < 0.05$ vs. GFP insulin ($n = 8$ per group). **B:** Quantitative bar graph of basal Ser1101 IRS-1 phosphorylation ($n = 4$). *** $P < 0.001$ vs. GFP. **C:** Quantitative bar graph of Ser473 Akt phosphorylation ($n = 11$). * $P < 0.05$, *** $P < 0.001$ vs. basal; # $P < 0.05$ vs. Ad-GFP. **D:** Representative blots of Ser1101 pIRS-1, total IRS-1, Ser473 pAkt, total Akt, and the loading control GAPDH in the presence (+) or absence (-) of 100 nmol/L of insulin in control myotubes (GFP) and myotubes overexpressing ATGL.

(Fig. 5A and B). Similarly, nonselective PKC inhibition fully rescued insulin-stimulated glycogen synthesis to control GFP levels in myotubes overexpressing ATGL (Fig. 5C). PKC inhibition by the nonselective inhibitor calphostin C (1 μ mol/L) was sufficient to fully rescue ATGL-mediated insulin resistance. ATGL-mediated inhibition of glycogen synthesis and Akt phosphorylation was not prevented by the de novo ceramide synthesis inhibitor myriocin (10 μ mol/L) (Supplementary Fig. 1).

HSL overexpression is sufficient to rescue ATGL-mediated insulin resistance. We tested the hypothesis that restoring a proper cellular lipolytic balance could reverse ATGL-mediated insulin resistance. To do so, we concomitantly overexpressed ATGL and HSL in differentiated myotubes and examined insulin signaling and action. HSL overexpression by itself did not produce lipotoxicity and insulin resistance (Supplementary Fig. 2). The concomitant overexpression of HSL and ATGL increased both HSL (3.4 ± 0.8 -fold, $P < 0.05$) and ATGL (3.2 ± 0.6 -fold, $P < 0.05$) protein content, TAGH activity (4.4 ± 2.0 -fold, $P < 0.01$), and DAGH activity (5.1 ± 1.8 -fold, $P < 0.01$). When coexpressed with ATGL, HSL was sufficient to completely rescue ATGL-mediated insulin resistance. This was evidenced by a full restoration of insulin-mediated Akt activation (Fig. 6A and B) and glycogen synthesis (Fig. 6C) to GFP control levels in myotubes coexpressing ATGL and HSL compared with ATGL alone.

Selective HSL inhibition impairs insulin signaling. We next examined the effect of HSL-selective inhibition by the BAY compound on DAG levels and insulin action. BAY has been shown to be a highly selective HSL inhibitor in previous studies (24). We observed a moderate increase in total DAG levels (+29%, $P = 0.068$) in myotubes treated for 24 h with 1 μ mol/L of BAY (Fig. 7A). BAY treatment did not increase ceramide content (0.57 ± 0.07 vs. 0.57 ± 0.06

nmol/mg for control and BAY, respectively). In the same treatment condition, BAY reduced Tyr612-IRS-1 phosphorylation on insulin treatment (-30% , $P < 0.05$) (Fig. 7B and C) and insulin-mediated Akt phosphorylation (-28% , $P = 0.03$) (Fig. 7B and D). We did not observe additive effects of ATGL overexpression combined with HSL inhibition compared with ATGL overexpression alone on insulin-stimulated Akt Ser473 phosphorylation (Supplementary Fig. 3).

DISCUSSION

Ectopic fat deposition in non-adipose tissues such as skeletal muscle is a common feature of insulin resistance in obesity and type 2 diabetes (3–5). The mechanisms underlying IMTG accumulation and elevated lipotoxicity in insulin-resistant states are not yet fully understood. We show for the first time a novel mechanism by which an altered lipolytic balance in skeletal muscle might contribute to lipotoxicity and insulin resistance in humans. An imbalance of ATGL relative to HSL promotes DAG accumulation and induces insulin resistance at least in part through a DAG/PKC pathway.

We first showed that ATGL protein expression in vastus lateralis samples obtained from a wide range of subjects was negatively associated with whole-body insulin sensitivity measured by euglycemic hyperinsulinemic clamp. It is interesting to note that the glucose disposal rate during this clamp is mostly accounted by skeletal muscle and thus mostly reflects skeletal muscle insulin sensitivity in lean subjects. Higher doses of insulin are required to fully suppress hepatic glucose production in obese and type 2 diabetic subjects as previously shown (34). Thus, the relationship between muscle ATGL and insulin sensitivity is stronger in lean subjects than in obese and type 2 diabetic

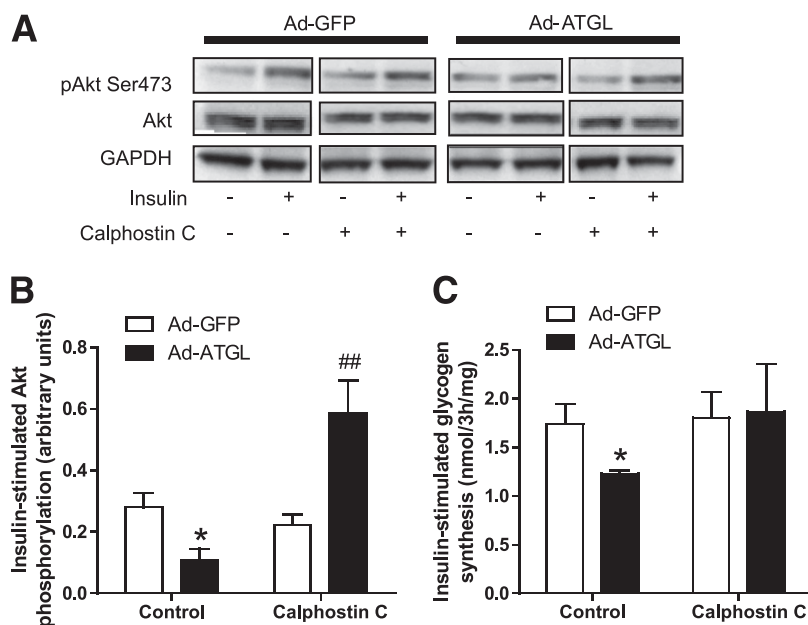


FIG. 5. ATGL-mediated insulin resistance involves PKC activation. **A:** Representative blots of Ser473 pAkt, total Akt, and GAPDH in the presence (+) or absence (-) of insulin and the nonselective PKC inhibitor calphostin C (1 μ mol/L) in control myotubes (GFP) and myotubes overexpressing ATGL. **B:** Quantitative bar graph of insulin-stimulated Ser473 Akt phosphorylation ($n = 3$); insulin-stimulated Akt phosphorylation was calculated as the Δ between basal and insulin stimulation in each condition. * $P < 0.05$ vs. GFP; ## $P < 0.01$ vs. GFP calphostin C. **C:** Insulin-stimulated glycogen synthesis in myotubes expressing GFP and ATGL in the absence (control) or presence of calphostin C. Glycogen synthesis was expressed as the Δ change between glycogen synthesis under insulin stimulation and glycogen synthesis at baseline. * $P < 0.05$ vs. GFP ($n = 4$).

subjects. When the data were examined by group, only obese type 2 diabetic subjects displayed increased muscle ATGL protein content. This finding is slightly in contrast with recent data showing an increased skeletal muscle ATGL protein expression in nondiabetic obese versus age-matched lean individuals (35). The discrepancy could be

explained by an effect of aging because the type 2 diabetic subjects were older than the lean and obese subjects in our study. Thus, age-related changes in skeletal muscle lipases with respect to insulin sensitivity should be further explored. Elevated muscle ATGL protein in obese type 2 diabetic subjects is in agreement with a higher muscle DAG

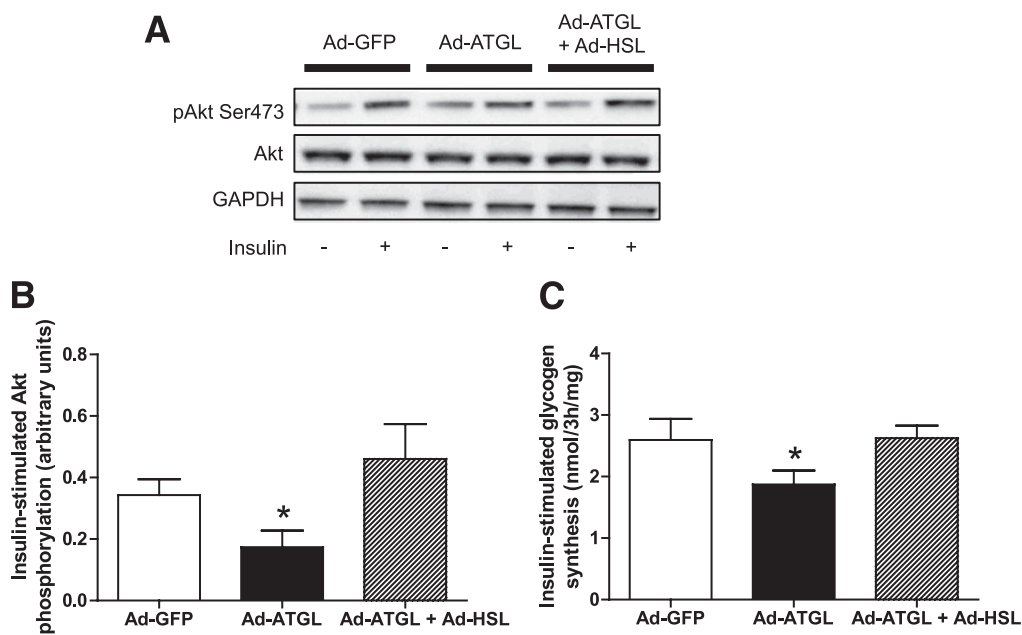


FIG. 6. Rescue of ATGL-mediated insulin resistance by HSL. **A:** Representative blots of Ser473 pAkt, total Akt, and GAPDH in the presence (+) or absence (-) of insulin in control myotubes (GFP) and myotubes overexpressing ATGL alone (Ad-ATGL) or in combination with HSL (Ad-ATGL+Ad-HSL). **B:** Quantitative bar graph of insulin-stimulated Ser473 Akt phosphorylation ($n = 4$); insulin-stimulated Akt phosphorylation was calculated as the Δ between basal and insulin stimulation in each condition. * $P < 0.05$ vs. GFP. **C:** Insulin-stimulated glycogen synthesis was measured in control myotubes (GFP) and myotubes overexpressing ATGL alone (Ad-ATGL) or in combination with HSL (Ad-ATGL+Ad-HSL). * $P < 0.05$ vs. GFP ($n = 6$).

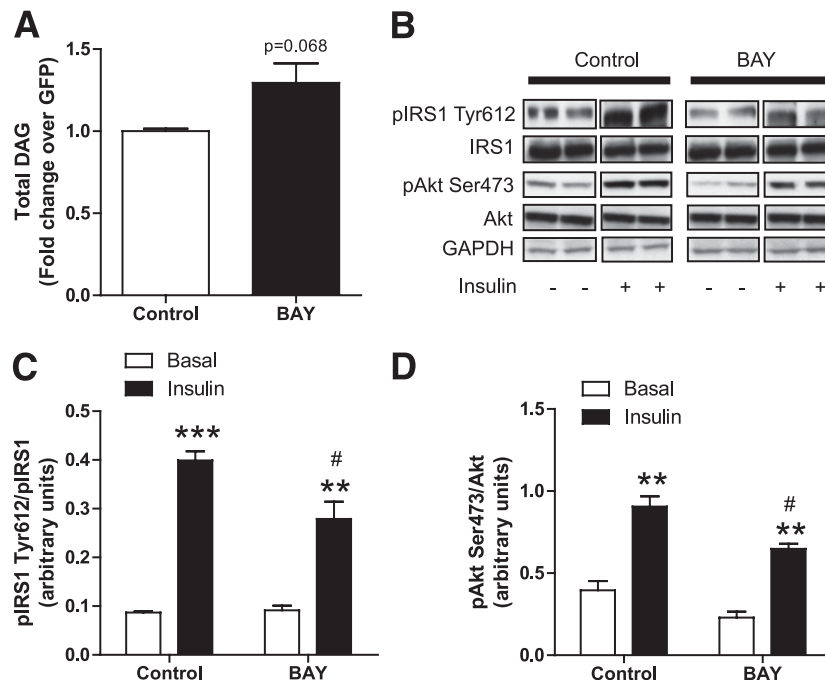


FIG. 7. Selective HSL inhibition disrupts insulin signaling. **A:** Total DAGs were measured in control myotubes and myotubes treated for 24 h with 1 $\mu\text{mol/L}$ of the selective HSL inhibitor BAY ($n = 6$). **B:** Representative blots of Tyr1162 pIR, total IRalpha, Ser473 pAkt, total Akt, and GAPDH in the presence (+) or absence (-) of insulin in control myotubes and myotubes treated with BAY. Quantitative bar graphs of **(C)** Tyr612-IRS-1 phosphorylation ($n = 4$) and **(D)** Ser473 Akt phosphorylation ($n = 4$) in control myotubes and myotubes treated with the BAY compound. ** $P < 0.01$; *** $P < 0.001$ vs. basal; # $P < 0.05$ vs. control insulin.

content previously reported in these subjects (36). We next evaluated the causal relationship between elevated ATGL expression and insulin resistance in primary culture of skeletal muscle cells.

We overexpressed ATGL in human primary myotubes using an adenovirus and assessed the consequences on lipids and insulin action. Elevated expression of ATGL reduced TAG content and simultaneously increased DAG and ceramide content. Ceramides are potentially produced de novo through the action of serine palmitoyl-transferase I as previously shown (8). ATGL-mediated lipotoxicity was paralleled by impairment in insulin-stimulated glycogen synthesis and insulin signaling possibly due to PKC-mediated Ser1101-IRS-1 phosphorylation and downstream inhibition of Akt Ser473 phosphorylation. Of note, increased ATGL expression induced baseline Akt Ser473 phosphorylation independently of insulin. This suggests that ATGL may activate potential regulators of Ser473 Akt, such as mTORC2, by yet unknown mechanisms (37). Future studies will be required to dissect the precise mechanism by which ATGL elicits baseline Akt activation. IRS-1 phosphorylation at Ser1101 is primarily mediated by PKC θ and induces general inhibition of IRS-1 function (13). Together, our data show that ATGL mediates insulin resistance at least in part through DAG and PKC activation. Itani et al. (38,39) have previously shown that membrane-associated PKC β and θ protein content and activity increased the skeletal muscle of obese versus lean and obese diabetic versus nondiabetic matched control subjects, respectively. Even if the exact nature of DAG stereoisomers produced by the action of ATGL is currently unknown, the data support an important role for DAG in mediating skeletal muscle insulin resistance in this model. This observation is consistent with other studies showing a critical role of DAG in mediating insulin resistance in liver (40) and skeletal

muscle (10–12) in response to high-fat diets and lipid infusions. Our results are also consistent with a study by Bell et al. (41) suggesting that AML12 liver cells lacking the lipid coat protein adipophilin and tail-interacting protein of 47 kDa develop insulin resistance with increased recruitment of ATGL to lipid droplets.

Of interest, ATGL-mediated insulin resistance was fully rescued by HSL after restoring a proper cellular lipolytic balance. Overexpression of HSL by itself did not cause lipotoxicity and insulin resistance contrary to ATGL. HSL displays a high DAG substrate specificity and is considered the major DAG hydrolase in several tissues (42). This supports the concept that the functional balance between ATGL and HSL may influence intracellular DAG concentrations and insulin action in skeletal muscle. Altogether, these data highlight a potential protective role of DAG hydrolases against intramyocellular lipotoxicity by their ability to rapidly hydrolyze DAG. The importance of DAG turnover in insulin resistance is also illustrated by the protective role of DGAT1 against intramyocellular lipotoxicity and fat-induced insulin resistance by increasing lipid partitioning into IMTG (43,44). Along these lines, reduced DAG kinase- δ activity, which converts DAG into phosphatidic acid, might also contribute to skeletal muscle insulin resistance by increasing total DAG level (45).

Consistent with recent studies that reported a robust reduction in skeletal muscle HSL protein expression in insulin-resistant obese subjects (35,46), our study confirmed that both HSL Ser660 phosphorylation and HSL protein content were reduced in skeletal muscle of obese compared with lean subjects. The trend for increased HSL protein content in skeletal muscle of patients with type 2 diabetes could be explained by the hyperglycemic milieu because glucose was shown to induce HSL transcription in adipocytes (47). To study the impact of reduced HSL

expression/activity in skeletal muscle, we next evaluated the consequences of inhibiting HSL activity on lipid pools and insulin sensitivity in myotubes. HSL activity is regulated by phosphorylation on serine residues in response to muscle contraction and catecholamines *in vivo* (48). Jocken et al. (46) found that reduced HSL phosphorylation at Ser563, Ser565, and Ser659 was entirely due to lower HSL protein content and associated with reduced resting glycerol release from the forearm muscle of obese subjects. We report that selective inhibition of HSL increases specifically total DAG levels and consequently disrupts insulin receptor signaling and action. This observation is somehow consistent with data on HSL knockout mice that are insulin-resistant at the level of the skeletal and cardiac muscles when fed a chow diet (49,50) and accumulate DAG in their muscles (16). Further studies will be required to unravel the precise mechanism by which reduced HSL expression/activity induces insulin resistance in skeletal muscle.

In conclusion, the current study highlights a new mechanism by which an altered lipolytic balance between ATGL and HSL induces DAG and insulin resistance in skeletal muscle. The molecular mechanism involves at least in part DAG-mediated PKC activation. Future studies should explore the cause-effect relationship between altered lipase expression and insulin resistance *in vivo* in animal models with targeted modulations of lipase expression in skeletal muscle. Targeting skeletal muscle lipases might be of potential therapeutic interest for improving insulin resistance in obesity and type 2 diabetes.

ACKNOWLEDGMENTS

This work was supported by grants from the National Research Agency (ANR-09-JCJC-0019-01) and the European Foundation for the Study of Diabetes/Novo Nordisk (to C.M.); the Commission of the European Communities (Integrated Project HEPADIP; <http://www.hepadip.org/>), Contract No. LSHM-CT-2005-018734 (to D.L.); and National Institutes of Health grants US-1P30-DK-072476 (Pennington Biomedical Research Center/Nutrition Obesity Research Center) and R01-AG-030226 (to S.R.S.). The Hormone Assay and Analytical Services Core, Vanderbilt Diabetes Research and Training Center, supported by National Institutes of Health Grant DK-20593, performed TAG and DAG analyses.

No potential conflicts of interest relevant to this article were reported.

P.-M.B., K.L., A.M., G.L., and G.S. researched data and reviewed and edited the article. A.C.R. reviewed and edited the article. S.R.S. and D.L. contributed to discussion and reviewed and edited the article. C.M. researched data and wrote the article.

The authors thank Diana Albarado (Pennington Biomedical Research Center, Baton Rouge, LA), Shantele Thomas (Burnham Institute, Winter Park, FL), and Maarten Coonen (Maastricht University, the Netherlands) for excellent technical assistance.

REFERENCES

- DeFronzo RA. Pathogenesis of type 2 diabetes mellitus. *Med Clin North Am* 2004;88:787–835, ix
- McGarry JD. Banting lecture 2001: dysregulation of fatty acid metabolism in the etiology of type 2 diabetes. *Diabetes* 2002;51:7–18
- Krssak M, Falk Petersen K, Dresner A, et al. Intramyocellular lipid concentrations are correlated with insulin sensitivity in humans: a ^1H NMR spectroscopy study. *Diabetologia* 1999;42:113–116
- Pan DA, Lillioja S, Kriketos AD, et al. Skeletal muscle triglyceride levels are inversely related to insulin action. *Diabetes* 1997;46:983–988
- Perseghin G, Scifo P, De Cobelli F, et al. Intramyocellular triglyceride content is a determinant of *in vivo* insulin resistance in humans: a ^1H - ^{13}C nuclear magnetic resonance spectroscopy assessment in offspring of type 2 diabetic parents. *Diabetes* 1999;48:1600–1606
- Unger RH. Minireview: weapons of lean body mass destruction: the role of ectopic lipids in the metabolic syndrome. *Endocrinology* 2003;144:5159–5165
- Adams JM 2nd, Pratipanawatr T, Berria R, et al. Ceramide content is increased in skeletal muscle from obese insulin-resistant humans. *Diabetes* 2004;53:25–31
- Chavez JA, Knotts TA, Wang LP, et al. A role for ceramide, but not diacylglycerol, in the antagonism of insulin signal transduction by saturated fatty acids. *J Biol Chem* 2003;278:10297–10303
- Holland WL, Brozinick JT, Wang LP, et al. Inhibition of ceramide synthesis ameliorates glucocorticoid-, saturated-fat-, and obesity-induced insulin resistance. *Cell Metab* 2007;5:167–179
- Dresner A, Laurent D, Marcucci M, et al. Effects of free fatty acids on glucose transport and IRS-1-associated phosphatidylinositol 3-kinase activity. *J Clin Invest* 1999;103:253–259
- Griffin ME, Marcucci MJ, Cline GW, et al. Free fatty acid-induced insulin resistance is associated with activation of protein kinase C θ and alterations in the insulin signaling cascade. *Diabetes* 1999;48:1270–1274
- Itani SI, Ruderman NB, Schmieder F, Boden G. Lipid-induced insulin resistance in human muscle is associated with changes in diacylglycerol, protein kinase C, and I κ B α . *Diabetes* 2002;51:2005–2011
- Li Y, Soos TJ, Li X, et al. Protein kinase C θ inhibits insulin signaling by phosphorylating IRS1 at Ser(1101). *J Biol Chem* 2004;279:45304–45307
- Timmers S, Schrauwen P, de Vogel J. Muscular diacylglycerol metabolism and insulin resistance. *Physiol Behav* 2008;94:242–251
- Langfort J, Ploug T, Ihlemann J, Saldo M, Holm C, Galbo H. Expression of hormone-sensitive lipase and its regulation by adrenaline in skeletal muscle. *Biochem J* 1999;340:459–465
- Haemmerle G, Zimmermann R, Hayn M, et al. Hormone-sensitive lipase deficiency in mice causes diglyceride accumulation in adipose tissue, muscle, and testis. *J Biol Chem* 2002;277:4806–4815
- Haemmerle G, Lass A, Zimmermann R, et al. Defective lipolysis and altered energy metabolism in mice lacking adipose triglyceride lipase. *Science* 2006;312:734–737
- Zimmermann R, Strauss JG, Haemmerle G, et al. Fat mobilization in adipose tissue is promoted by adipose triglyceride lipase. *Science* 2004;306:1383–1386
- Ukropcova B, McNeil M, Sereda O, et al. Dynamic changes in fat oxidation in human primary myocytes mirror metabolic characteristics of the donor. *J Clin Invest* 2005;115:1934–1941
- Listenberger LL, Han X, Lewis SE, et al. Triglyceride accumulation protects against fatty acid-induced lipotoxicity. *Proc Natl Acad Sci U S A* 2003;100:3077–3082
- Turpin SM, Lancaster GI, Darby I, Febbraio MA, Watt MJ. Apoptosis in skeletal muscle myotubes is induced by ceramides and is positively related to insulin resistance. *Am J Physiol Endocrinol Metab* 2006;291:E1341–E1350
- Pickersgill L, Litherland GJ, Greenberg AS, Walker M, Yeaman SJ. Key role for ceramides in mediating insulin resistance in human muscle cells. *J Biol Chem* 2007;282:12583–12589
- Hessvik NP, Bakke SS, Fredriksson K, et al. Metabolic switching of human myotubes is improved by n-3 fatty acids. *J Lipid Res* 2010;51:2090–2104
- Langin D, Dicker A, Tavernier G, et al. Adipocyte lipases and defect of lipolysis in human obesity. *Diabetes* 2005;54:3190–3197
- Bergstrom J. Percutaneous needle biopsy of skeletal muscle in physiological and clinical research. *Scand J Clin Lab Invest* 1975;35:609–616
- DeFronzo RA, Tobin JD, Andres R. Glucose clamp technique: a method for quantifying insulin secretion and resistance. *Am J Physiol* 1979;237:E214–E223
- Mairal A, Langin D, Arner P, Hoffstedt J. Human adipose triglyceride lipase (PNPLA2) is not regulated by obesity and exhibits low *in vitro* triglyceride hydrolase activity. *Diabetologia* 2006;49:1629–1636
- Folch J, Lees M, Sloane Stanley GH. A simple method for the isolation and purification of total lipides from animal tissues. *J Biol Chem* 1957;226:497–509
- Morrison WR, Smith LM. Preparation of fatty acid methyl esters and dimethylacetals from lipids with boron fluoride-methanol. *J Lipid Res* 1964;5:600–608
- Liebisch G, Drobnik W, Reil M, et al. Quantitative measurement of different ceramide species from crude cellular extracts by electrospray

- ionization tandem mass spectrometry (ESI-MS/MS). *J Lipid Res* 1999;40:1539–1546
31. Bligh EG, Dyer WJ. A rapid method of total lipid extraction and purification. *Can J Biochem Physiol* 1959;37:911–917
 32. Liebisch G, Lieser B, Rathenberg J, Drobnik W, Schmitz G. High-throughput quantification of phosphatidylcholine and sphingomyelin by electrospray ionization tandem mass spectrometry coupled with isotope correction algorithm. *Biochim Biophys Acta* 2004;1686:108–117
 33. Schmitz-Peiffer C, Biden TJ. Protein kinase C function in muscle, liver, and beta-cells and its therapeutic implications for type 2 diabetes. *Diabetes* 2008;57:1774–1783
 34. Bonadonna RC, Groop L, Kraemer N, Ferrannini E, Del Prato S, DeFronzo RA. Obesity and insulin resistance in humans: a dose-response study. *Metabolism* 1990;39:452–459
 35. Jocken JW, Moro C, Goossens GH, et al. Skeletal muscle lipase content and activity in obesity and type 2 diabetes. *J Clin Endocrinol Metab* 2010;95:5449–5453
 36. Moro C, Galgani JE, Luu L, et al. Influence of gender, obesity, and muscle lipase activity on intramyocellular lipids in sedentary individuals. *J Clin Endocrinol Metab* 2009;94:3440–3447
 37. Huang J, Manning BD. A complex interplay between Akt, TSC2 and the two mTOR complexes. *Biochem Soc Trans* 2009;37:217–222
 38. Itani SI, Pories WJ, Macdonald KG, Dohm GL. Increased protein kinase C theta in skeletal muscle of diabetic patients. *Metabolism* 2001;50:553–557
 39. Itani SI, Zhou Q, Pories WJ, MacDonald KG, Dohm GL. Involvement of protein kinase C in human skeletal muscle insulin resistance and obesity. *Diabetes* 2000;49:1353–1358
 40. Neschen S, Morino K, Dong J, et al. n-3 Fatty acids preserve insulin sensitivity in vivo in a peroxisome proliferator-activated receptor-alpha-dependent manner. *Diabetes* 2007;56:1034–1041
 41. Bell M, Wang H, Chen H, et al. Consequences of lipid droplet coat protein downregulation in liver cells: abnormal lipid droplet metabolism and induction of insulin resistance. *Diabetes* 2008;57:2037–2045
 42. Holm C. Molecular mechanisms regulating hormone-sensitive lipase and lipolysis. *Biochem Soc Trans* 2003;31:1120–1124
 43. Liu L, Zhang Y, Chen N, Shi X, Tsang B, Yu YH. Upregulation of myocellular DGAT1 augments triglyceride synthesis in skeletal muscle and protects against fat-induced insulin resistance. *J Clin Invest* 2007;117:1679–1689
 44. Schenk S, Horowitz JF. Acute exercise increases triglyceride synthesis in skeletal muscle and prevents fatty acid-induced insulin resistance. *J Clin Invest* 2007;117:1690–1698
 45. Chibalin AV, Leng Y, Vieira E, et al. Downregulation of diacylglycerol kinase delta contributes to hyperglycemia-induced insulin resistance. *Cell* 2008;132:375–386
 46. Jocken JW, Roepstorff C, Goossens GH, et al. Hormone-sensitive lipase serine phosphorylation and glycerol exchange across skeletal muscle in lean and obese subjects: effect of beta-adrenergic stimulation. *Diabetes* 2008;57:1834–1841
 47. Smith F, Rouet P, Lucas S, et al. Transcriptional regulation of adipocyte hormone-sensitive lipase by glucose. *Diabetes* 2002;51:293–300
 48. Jocken JW, Blaak EE. Catecholamine-induced lipolysis in adipose tissue and skeletal muscle in obesity. *Physiol Behav* 2008;94:219–230
 49. Park SY, Kim HJ, Wang S, et al. Hormone-sensitive lipase knockout mice have increased hepatic insulin sensitivity and are protected from short-term diet-induced insulin resistance in skeletal muscle and heart. *Am J Physiol Endocrinol Metab* 2005;289:E30–E39
 50. Mulder H, Sörhede-Winzell M, Contreras JA, et al. Hormone-sensitive lipase null mice exhibit signs of impaired insulin sensitivity whereas insulin secretion is intact. *J Biol Chem* 2003;278:36380–36388